

A Selective Stepwise Heme Oxygenase Model System: An Iron(IV)-Oxo Porphyrin π -Cation Radical Leads to a Verdoheme-Type Compound via an Isoporphyrin Intermediate

Isaac Garcia-Bosch, Savita K. Sharma, and Kenneth D. Karlin*

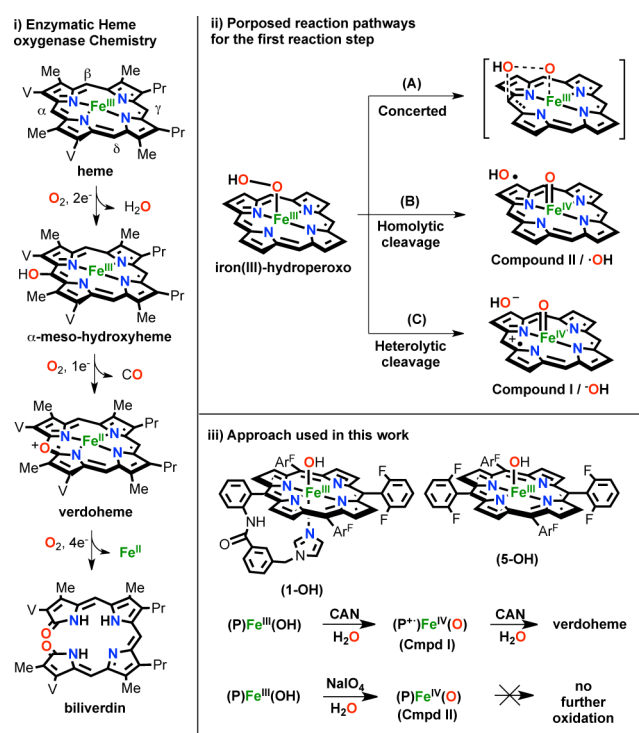
Department of Chemistry, The Johns Hopkins University, Baltimore, Maryland 21218, United States

S Supporting Information

ABSTRACT: The selective oxidation of the α -position of two heme-Fe^{III} tetraarylporphyrinate complexes occurs when water(hydroxide) attacks their oxidized Cmpd I-type equivalents, high-valent Fe^{IV}=O π -cation radical species ((P^{•+})Fe^{IV}=O). Stepwise intermediate formation occurs, as detected by UV-vis spectroscopic monitoring or mass spectrometric interrogation, being iron(III) isoporphyrins, iron(III) benzoyl-biliverdins, and the final verdoheme-like products. Heme oxygenase (HO) enzymes could proceed through heterolytic cleavage of an iron(III)-hydroperoxo intermediate to form a transient Cmpd I-type species.

Heme oxygenase (HO) is an enzyme that catalyzes the conversion of free heme to free iron, carbon monoxide, and biliverdin. This process is biologically important because: (i) HO degrades free heme, which itself is highly toxic; (ii) it facilitates the recycling of iron and therefore contributes to iron homeostasis; hemes comprise the major source of this metal in the body (97%); (iii) the heme degradation produces carbon monoxide, generating 87% of the CO found in the body; this recently being established to be a small molecule cellular signaling agent; and (iv) the eventual reaction product is biliverdin, which is reduced to bilirubin, a molecule with antioxidant properties.¹ The oxidation of heme is a very intricate process, utilizing three molecules of molecular oxygen and seven reducing equivalents, over three consecutive oxygenation steps (Scheme 1, left). In the first stage, the porphyrin α -meso carbon is selectively hydroxylated, and one O₂ molecule and two electrons are consumed. The second step is a fast autooxidation, with release of carbon monoxide and formation of verdoheme, consuming another O₂ and one electron. The last step is thought to be the rate-limiting step, requiring four electrons and another molecule of O₂, generating biliverdin and Fe²⁺. Although it is commonly proposed that an iron(III)-hydroperoxo species is the active oxidizing agent in both the first and third steps, the reaction mechanism has been debated and is not fully understood. Analysis of the crystal structure of ferrous-O₂ heme-HmuO from bacteria showed an interaction between the dioxygen derived ligand with a water cluster localized between Tyr53, Asp136, and Arg132 residues.^{1d} The position of this water cluster suggests that it is involved in the mechanism, specifically directing the Fe(III)-OOH selective attack to the α -meso carbon. However, experimental and DFT calculations give contradictory results

Scheme 1. (i) Enzymatic HO Chemistry; (ii) Proposed Reaction Pathways for the First Heme Hydroxylation; and (iii) Approach Used in This Work



concerning exactly how the attack of this ferric-hydroperoxo complex occurs.

Three main mechanistic scenarios have been proposed (Scheme 1, top right): the first (A) is proposed by Ikeda-Saito, Hoffman and co-workers by the study of the intermediates generated during HO catalytic cycle, and it entails concerted attack of the distal oxygen of a Fe^{III}-OOH, where O-O bond cleavage and C-O bond formation occur simultaneously.² The other two possible pathways are proposed by DFT calculations from the Shaik and Yoshizawa groups, respectively, and they involve prior O-O bond scission. Pathway (B) involves generation of Fe^{IV}=O (Cmpd II) plus hydroxyl radical, which is directed by H-bonding to selectively attack the α -meso carbon.³ Pathway (C) generates a Fe^{IV}=O π -

Received: June 8, 2013

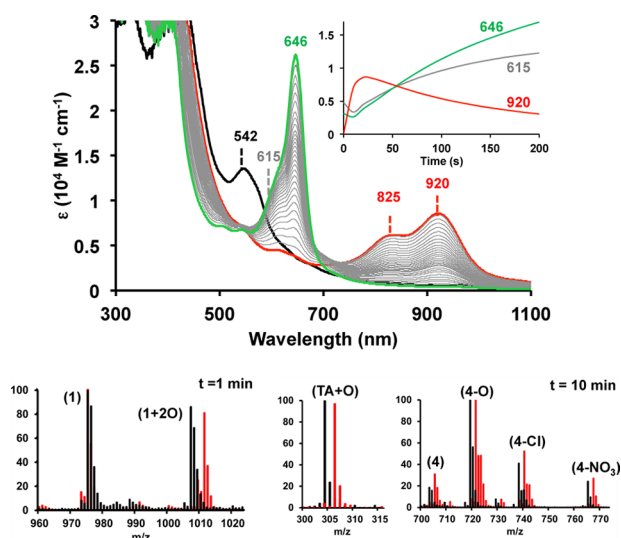


Figure 1. Top: UV-vis spectroscopic changes occurring during the oxidation of complex (1-OH) [0.1 mM] with CAN [40 mM]. Initial (1-OH) (black), isoporphyrin complex (2) (red; $t = 10$ s) and final verdoheme-type complex (4-X) (green; $t = 300$ s). The gray spectra show the formation of a verdoheme-type complex (4-X) from the isoporphyrinic intermediate (2) via complex (3) (broad band centered at 615 nm). Inset plot: Abs. evolution over time at different wavelength values. Bottom: ESI-MS spectra for the oxidation of (1-OH) [0.1 mM] with CAN [10 mM] in $\text{CH}_3\text{CN}/\text{H}_2\text{O}$ (1:1) (black) or $\text{CH}_3\text{CN}/\text{H}_2^{18}\text{O}$ (1:1) mixture (red) after 1 min of addition of oxidant (left) and after 10 min (right).⁹

cation radical (Cmpd I) and hydroxide; the latter attacks the heme α -position as a nucleophile, leading to overall porphyrin hydroxylation.⁴

While there exists extensive investigations on the natural systems under both stoichiometric and catalytic conditions, HO model systems are rare, excepting the highly notable work of Balch and co-workers.⁵ They employed a “coupled oxidation” approach, using O_2 with a sacrificial reductant to stepwise convert an octaethylporphyrin (OEP) iron(II) complex to its *meso*-hydroxylated iron-porphyrin, verdoheme, and biliverdin analog products (Scheme 1, left). Broad descriptions of the reaction products were provided, although the detection and characterization of any reaction intermediates such as a Fe^{III} -OOH or high valent $\text{Fe}^{\text{IV}}=\text{O}$ species were not reported. Herein, we present a fresh approach toward understanding reaction pathways which may be involved in HO-type oxidative chemistry, as outlined in Scheme 1 (right bottom): (a) a heme with covalently tethered imidazole as axial ligand base ($\text{P}^{\text{Im}}\text{Fe}^{\text{III}}(\text{OH})$ (1-OH) and the related heme ($\text{F}_8\text{Fe}^{\text{III}}(\text{OH})$ (5-OH), where all *meso*-positions are protected with aromatic moieties, are employed, and (b) cerium(IV) ammonium nitrate (CAN) or sodium periodate (NaIO_4) are used as sacrificial oxidants and water is the oxygen atom source. CAN and NaIO_4 have been widely used to generate high-valent metal species.^{6a} Reaction between metal ions and these oxidants has been used not only for characterization purposes but also in water oxidation to dioxygen and substrate oxidation chemistries. For example, Fukuzumi, Nam and co-workers used CAN in the presence of H_2O to generate a nonheme Mn^{IV} -oxo species, and the oxygen atom from water was found to reside in resulting oxygenated alkane or alkene substrates.^{6b} In the chemistry described here, these strong oxidants are used to generate high-valent oxo-iron species (Cmpd I, ($\text{P}^{\text{Im}}\text{Fe}^{\text{IV}}=\text{O}$ or Cmpd II,

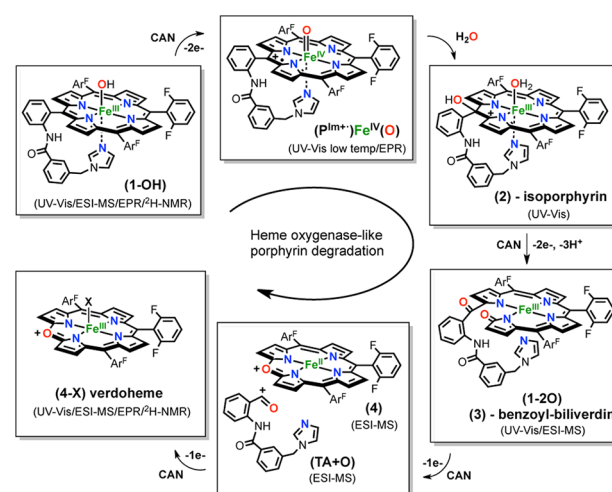


Figure 2. Proposed mechanism for the selective oxidation of (1-OH) with CAN to verdoheme complex (4-X) via formation of intermediates ($\text{P}^{\text{Im}}\text{Fe}^{\text{IV}}=\text{O}$), isoporphyrin (2), and benzoyl-biliverdin (3). Drawings for analogs produced in the chemistry of (5-OH) are given in the Scheme S1. EPR and ^1H NMR data for complexes (1-OH; see SI), (5-OH; high-spin Fe^{III}), (4-X; high-spin Fe^{III}) generated in the crude reaction mixture (i.e., in situ) and for the isolated (4-X; high-spin Fe^{III}) were also obtained (See SI).

($\text{P}\text{Fe}^{\text{IV}}=\text{O}$ synthetic analogs) in order to evaluate their possible roles in heme intramolecular oxidation processes.

Reaction of a ($\text{P}^{\text{Im}}\text{Fe}^{\text{III}}(\text{OH})$ (1-OH) solution (0.1 mM, in $\text{CH}_3\text{CN}/\text{H}_2\text{O}$ (1:1) at 0°C) with excess of CAN [40 mM] was followed by UV-vis spectroscopy. Absorbance ascribed to (1-OH) ($\lambda_{\text{max}} = 542$ nm, $\epsilon = 13000$ $\text{M}^{-1}\text{cm}^{-1}$) immediately changed, generating a new species (2: $\lambda_{\text{max}} = 825$ nm, $\epsilon = 6000$ $\text{M}^{-1}\text{cm}^{-1}$; $\lambda_{\text{max}} = 920$ nm, $\epsilon = 8500$ $\text{M}^{-1}\text{cm}^{-1}$) (Figure 1). This spectrum, while peculiar, is in fact highly characteristic of an iron(III)-isoporphyrin complex, which is two oxidation states above the $\text{Fe}(\text{III})$ -porphyrinate (also see below, Figure 2).⁷ Over time, the isoporphyrinic species (2) converted to another new species (3) with broad band UV-vis features centered at 615 nm, which further evolved to the final bright-green product species (4-X: $\lambda_{\text{max}} = 646$ nm, $\epsilon = 28000$ $\text{M}^{-1}\text{cm}^{-1}$). All transformations exhibited isosbestic behavior, suggesting clean stepwise transformations between each species involved. The UV-vis features of (4-X) are characteristic of a verdoheme-type complex (with α -*meso* O-atom instead of C-atom; also, see Figure 2), that are widely described in the literature.^{5,8} For comparison, oxidation of ($\text{F}_8\text{Fe}^{\text{III}}(\text{OH})$ (5-OH) with CAN was also performed (Figure S1). Analogous to (1-OH), this effected (5-OH) conversion to the same final verdoheme-type species (4-X). A solid final verdoheme product (4-X) was isolated and characterized by elemental analysis, UV-vis (matching literature verdohemes) spectroscopies, and ESI-MS (Figure 2), confirming its formulation. EPR spectroscopy confirmed that the (4-X) product is a high-spin iron(III), this spin state was also observed for the verdoheme-like species described by Balch and co-workers.⁵ A similar isoporphyrinic intermediate (2- F_8 , $\lambda_{\text{max}} = 930$ nm) evolved to a compound with a broad band centered at 615 nm (3- F_8), suggesting similar oxidation pathways occur for both Scheme 1 heme compounds (see Scheme S1).

ESI-MS experiments (Figure 1, bottom) provide corroborating evidence for our assignments for intermediates generated during the oxidation of ($\text{P}^{\text{Im}}\text{Fe}^{\text{III}}(\text{OH})$ (1-OH) and (F_8)-

$\text{Fe}^{\text{III}}(\text{OH})$ (**5-OH**). Different batches of the crude reaction mixtures were injected at different stages of the reaction (at time points: 0, 1, 5, 10, and 30 min) and were monitored to catch the evolution of different ions present. To aid the characterization, labeling experiments using H_2^{18}O and $^{18}\text{O}_2$ were also performed. Our assignments for ESI-MS peaks and complex structures are given in the proposed mechanistic scheme (Figure 2). Thus, explanations for the assignments are made throughout this presentation. For chemistry associated with $(\text{P}^{\text{III}})\text{Fe}^{\text{III}}(\text{OH})$ (**1-OH**), 1 min after addition of CAN [10 mM] two main peaks were detected corresponding to the $(\text{P}^{\text{III}})\text{Fe}(\text{III})$ complex (**1**) with loss of $-\text{OH}$; ($\text{C}_{55}\text{H}_{31}\text{F}_6\text{FeN}_7\text{O}^+$, $m/z = 975.2$) and a new species (**1 + 2O**, **3** in Figure 3) ($\text{C}_{55}\text{H}_{31}\text{F}_6\text{FeN}_7\text{O}_3^+$, $m/z = 1007.2$). When a $\text{CH}_3\text{CN}:\text{H}_2^{18}\text{O}$ (1:1) mixture was used as solvent, the peak observed now showed incorporation of two ^{18}O labeled atoms (**1 + 2 ^{18}O**) ($\text{C}_{55}\text{H}_{31}\text{F}_6\text{FeN}_7^{16}\text{O}^{18}\text{O}_2^+$, $m/z = 1011.2$); the two atoms in (**1 + 2O**) derive from water. After 5 min of reaction, the intensity of the peaks corresponding to (**1**) and (**1 + 2O**) decreased, and two sets of new peaks appeared at 703.1, 719.1, 738.1, and 765.1, well matching assignments to the verdoheme-type complex (**4**), ($\text{C}_{37}\text{H}_{17}\text{F}_6\text{FeN}_4\text{O}^+$, $m/z = 703.1$) but possessing various axial ligand ions (**4-X**) ($\text{X} = \text{O}^{2-}$, Cl^- , NO_3^-).⁹

To our surprise, the fragment corresponding to the cleavage of the tethered arm (**TA+O**, Figure 2) was also detected ($\text{C}_{18}\text{H}_{14}\text{N}_3\text{O}_2^+$, $m/z = 304.1$), and curiously, the mass peak suggested that it contained the *meso*-carbon atom from the porphyrin, ruling out both C–C cleavage of the *meso*-carbon and aryl group and C=O release (as carbon monoxide) derived from *meso*-carbon oxidation. Labeling experiments using H_2^{18}O , confirmed the formulation of the verdoheme-type species, showing incorporation of ^{18}O (>90%) into (**4 ^{18}O**) ($\text{C}_{37}\text{H}_{17}\text{F}_6\text{FeN}_4^{18}\text{O}$, $m/z = 705.1$), (**4 ^{18}O -X**, (721.1, 740.1, 767.1) and also the cleaved tethered arm (**TA+ ^{18}O** , Figure 2). After 10 min reaction time, residual amounts of (**1**) and (**1 + 2O**) were observed, and only peaks corresponding to (**4-X**) and (**TA+O**) were present. This observation is in agreement with the UV–vis disappearance of the isoporphyrin complex (**2**) (Figure 1) and sequential formation of benzoyl-biliverdin intermediate (**3**) and cleaved complex product (**4**). ESI-MS experiments were also carried out under an $^{18}\text{O}_2$ atmosphere, and there was no incorporation of labeled ^{18}O -oxygen into any species, confirming the water as the oxygen source (see SI). As found for (**1-OH**), ESI-MS monitoring of the oxidation of (**5-OH**) (Scheme 1) indicated the formation of the verdoheme-type complex (**4-X**), also ratifying corresponding UV–vis spectroscopic experiments (see SI). However, no intermediate species were observed, probably due to their lower stability caused by the higher concentration of CAN needed. As expected, no fragment corresponding to the tethered arm (**TA+O**) was observed.

To shed further light on the reaction mechanism, kinetic experiments for the oxidation of (**1-OH**) and (**5-OH**) were performed at different CAN concentrations [5–100 mM] (kinetic traces and reaction rates are given in the SI). For both complexes, there was a clear dependence between the CAN concentration and the rates of formation and decay of the first isoporphyrin species (compounds (**2**) and (**2-F₈**)) as well as the formation of complex (**4**). Some differences were observed when comparing the behavior of (**1-OH**) vs (**5-OH**). Lower concentrations of CAN [20–40 mM] were required for the full conversion of (**1-OH**) to verdoheme-type (**4-X**) compared to

complex (**5-OH**), where [80–100 mM] was needed. The higher reactivity of complex (**1-OH**) was also reflected in its higher reaction rates in all reaction steps (~5 times faster) compared to the ones shown by (**5-OH**). On the other hand, when complexes (**1-OH**) and (**5-OH**) were exposed to sodium periodate (NaIO_4), generation of metastable $(\text{P})\text{Fe}^{\text{IV}}=\text{O}$ complexes (Cmpd II-type) were observed by UV–vis (characteristic 540–555 nm bands) with no further oxidation of the porphyrin (see SI).¹⁰ This behavior implicates a more reactive species, a $(\text{P}^{+\bullet})\text{Fe}^{\text{IV}}=\text{O}$ (Cmpd I-type) species, as being required to effect *meso* position oxidation chemistry.

Fujii and co-workers^{7a} very recently demonstrated that an isoporphyrin complex is the reactive agent in the chlorination of aromatic compounds and olefins, being generated by nucleophilic attack of chloride to a $(\text{P}^{+\bullet})\text{Fe}^{\text{IV}}=\text{O}$ complex via formation of a dication species. Our kinetic experiments support the formation of a Cmpd I-like complex during the rate-determining step, prior to the nucleophilic attack of water to generate the isoporphyrinic intermediate.^{11a,b} The fact that complex (**1-OH**) needs less excess of CAN [20–40 mM] than complex (**5-OH**) [80–100 mM] also enforces this hypothesis, due to the lower redox potential (–0.1 to –0.2 V) shown by $(\text{P}^{+\bullet})\text{Fe}^{\text{IV}}=\text{O}$ complexes with imidazoles as axial bases compared with other anionic axial ligands (NO_3^- , ClO_4^- , e.g.).¹² Direct support for our hypothesis that a $(\text{P}^{+\bullet})\text{Fe}^{\text{IV}}=\text{O}$ species forms in the first reaction step was obtained by low-temperature experiments (–80 °C). In the reaction of the iron(III) complexes (**1-SbF₆**) and (**5-SbF₆**) with *m*CPBA (5 equiv) in a dichloromethane/water mixture (97:3 v:v), generation of Cmpd I $(\text{P}^{+\bullet})\text{Fe}^{\text{IV}}=\text{O}$ species was observed. The presence of water caused rapid transformation of this intermediate to the same isoporphyrin species (**2**) and (**2-F₈**) observed in the oxidation of (**1-OH**) and (**5-OH**), respectively, with CAN, consistent with the formation of the same $(\text{P}^{+\bullet})\text{Fe}^{\text{IV}}=\text{O}$ species under the two varying reaction conditions. Similarly, tetramethylammonium hydroxide can also act as a nucleophile, causing the formation of the same isoporphyrinic species (**2**) and (**2-F₈**) (UV–vis criterion) after generation of the respective Cmpd I-like species (Figures S5–S6).^{11c} Ortiz de Montellano and co-workers have studied the human HO-1 oxidation of substituted α - and γ -phenyl hemes and where oxidation of the α -*meso* position was observed without concomitant formation of CO (as is observed here). They proposed the oxidation of the α -phenyl substituted heme, via formation of an isoporphyrin complex, with similar UV–vis features observed here for oxidation of (**1-OH**).^{13b} In our case, UV–vis experiments clearly demonstrate the formation of an isoporphyrin complex. However, this intermediate is not detected by ESI-MS, probably due to its reduction during ionization. On the other hand, ESI-MS spectra have shown (vide supra) the formation of (**1 + 2O**) previous to the formation of the final verdoheme-type species. We propose a mechanism where (**1 + 2O**) is formulated as a benzoyl-biliverdin complex (**3**),¹⁴ formed by oxidation of isoporphyrin (**2**) (Figure 2). This benzoyl-biliverdin product was also observed in the enzymatic oxidation of α -phenyl heme, and its UV–vis features were similar to those observed in the conversion of (**2**) to (**4-X**) ($\lambda \cong 600\text{--}700\text{ nm}$). The one-electron oxidation of complex (**3**) leads to the formation of the verdoheme-type complex (**4**) and cleavage of the tethered arm (**TA + O**) in a benzaldehyde or benzoic acid form, maintaining the *meso* carbon in its structure. A similar mechanism was also proposed in the enzymatic catalysis, where benzoic acid was

detected during the oxidation of α -phenyl heme without release of CO, a pathway also proposed by Sarkar and co-workers in the decomposition of an isolated *meso*-hydroxylated iron(III) porphyrin to a verdoheme-type species.^{7b}

The present study clearly implicates Cmpd I formation, followed by *meso*-position nucleophilic water/hydroxide attack, leading to a HO-like verdoheme product, at least for the synthetic system employed. Whether or not this extends to one or more of the biological HO family cannot, of course, be stated. As mentioned, Ikeda-Saito and co-workers specifically ruled out the involvement of Cmpd I in the catalytic cycle of mammalian HO, by generation of this species with mCPBA and following its decay to a Cmpd II analog and not the verdoheme complex.^{2c} However, our experimental results support the Yoshizawa and co-workers proposal, where O–O heterolytic cleavage occurs generating Cmpd I, which assists water attack to the α -*meso* position.⁴ Moreover, it is in agreement with the secondary kinetic isotope effect observed in the enzyme upon deuteration of heme *meso* positions that suggests an sp^3 to sp^2 hybridization change occurs in the rate-determining step and with the solvent isotopic experiments observed ($(H_2O/D_2O) = 2.5$), where water acts as a proton source.^{2b} Our results are also in agreement with the Nakajima and Yamazaki observations where Cmpd I horseradish peroxidase C converts to a verdohemoprotein.¹⁵ There, an intermediate with UV–vis features (940–965 nm) was detected, very similar to the isoporphyrin formed in our systems and in Montellano's enzymatic catalysis. Moreover, in a recent report on a new family of HO (IsdG), formation of formaldehyde instead of CO was observed, similar to the observed (TA + O) product reported herein, which would suggest a similar reaction mechanism to the one described in the present work.¹⁶ Taken together, our new findings and many of the biochemical observations suggest that further consideration for the involvement of Cmpd I in the HO reaction pathway is required.

■ ASSOCIATED CONTENT

● Supporting Information

Figures S1–S33, Scheme S1, Tables S1–S2 and experimental details. This material is available free of charge via the Internet at <http://pubs.acs.org>.

■ AUTHOR INFORMATION

Corresponding Author

karlin@jhu.edu

Notes

The authors declare no competing financial interest.

■ ACKNOWLEDGMENTS

This research was supported by the USA National Institutes of Health (GM60353 to K.D.K.). I.G.B. thanks the European Commission for a Marie Curie International Outgoing Fellowship.

■ REFERENCES

- (1) (a) Ortiz de Montellano, P. R. *Acc. Chem. Res.* **1998**, *31*, 543. (b) Colas, C.; Ortiz de Montellano, P. R. *Chem. Rev.* **2003**, *103*, 2305. (c) Matsui, T.; Unno, M.; Ikeda-Saito, M. *Acc. Chem. Res.* **2010**, *43*, 240. (d) Unno, M.; Matsui, T.; Chu, G. C.; Couture, M.; Yoshida, T.; Rousseau, D. L.; Olson, J. S.; Ikeda-Saito, M. *J. Biol. Chem.* **2004**, *279*, 21055.
- (2) (a) Davydov, R. M.; Yoshida, T.; Ikeda-Saito, M.; Hoffman, B. M. *J. Am. Chem. Soc.* **1999**, *121*, 10656. (b) Davydov, R.; Matsui, T.; Fujii,

H.; Ikeda-Saito, M.; Hoffman, B. M. *J. Am. Chem. Soc.* **2003**, *125*, 16208. (c) Matsui, T.; Kim, S. H.; Jin, H.; Hoffman, B. M.; Ikeda-Saito, M. *J. Am. Chem. Soc.* **2006**, *128*, 1090.

(3) (a) Kumar, D.; de Visser, S. P.; Shaik, S. *J. Am. Chem. Soc.* **2005**, *127*, 8204. (b) Chen, H.; Moreau, Y.; Derat, E.; Shaik, S. *J. Am. Chem. Soc.* **2008**, *130*, 1953.

(4) (a) Kamachi, T.; Shestakov, A. F.; Yoshizawa, K. *J. Am. Chem. Soc.* **2004**, *126*, 3672. (b) Kamachi, T.; Yoshizawa, K. *J. Am. Chem. Soc.* **2005**, *127*, 10686. (c) Kamachi, T.; Nishimi, T.; Yoshizawa, K. *Dalton Trans.* **2012**, *41*, 11642.

(5) (a) Koerner, R.; Latos-Grazynski, L.; Balch, A. L. *J. Am. Chem. Soc.* **1998**, *120*, 9246. (b) Nguyen, K. T.; Rath, S. P.; Latos-Grazynski, L.; Olmstead, M. M.; Balch, A. L. *J. Am. Chem. Soc.* **2004**, *126*, 6210. (c) Rath, S. P.; Kalish, H.; Latos-Grazynski, L.; Olmstead, M. M.; Balch, A. L. *J. Am. Chem. Soc.* **2004**, *126*, 646.

(6) (a) Javier, J. C.; Ming-Kang, T.; Muckerman, J. T.; Meyer, T. J. *J. Am. Chem. Soc.* **2010**, *132*, 1545. (b) Sawant, S. C.; Wu, X.; Cho, J.; Cho, K.-B.; Kim, S. H.; Seo, M. S.; Lee, Y.-M.; Kubo, M.; Ogura, T.; Shaik, S.; Nam, W. *Angew. Chem., Int. Ed.* **2010**, *49*, 8190.

(7) (a) Cong, Z.; Kurahashi, T.; Fujii, H. *J. Am. Chem. Soc.* **2012**, *134*, 4469. (b) Abhilash, G. J.; Bhuyan, J.; Singh, P.; Maji, S.; Pal, K.; Sarkar, S. *Inorg. Chem.* **2009**, *48*, 1790.

(8) Sano, S.; Sano, T.; Morishima, I.; Shiro, Y.; Maeda, Y. *Proc. Natl. Acad. Sci. U.S.A.* **1986**, *83*, 531.

(9) (a) Nitrate counteranion is derived from CAN. Labelling experiments using $H_2^{18}O$ suggest that the mass corresponding to ($4^{18}O-O$) (O^{2-} as axial ligand) is generated in the ESI-MS ionization process by cleavage of ($4^{18}O-NO_3$). (b) As for labeling, we use “+” when incorporation of oxygen into the ligand structure was observed, e.g., intermediate (1 + 2O). We use “–” to indicate that the molecule observed acts as a counteranion or axial base, e.g., in the starting material (1-OH) or the final verdoheme-like products (4-X).

(10) (a) Nam, W.; Park, S.-E.; Lim, I. K.; Lim, M. H.; Hong, J.; Kim, K. *J. Am. Chem. Soc.* **2003**, *125*, 14674. (b) Ghiladi, R. A.; Kretzer, R. M.; Guzei, I.; Rheingold, A. L.; Neuhold, Y.-M.; Hatwell, K. R.; Zuberbühler, A. D.; Karlin, K. D. *Inorg. Chem.* **2001**, *40*, 5754.

(11) (a) As suggested by a reviewer, we considered that the first oxidation step for the oxidation of (1-OH) could proceed via direct attack of the Ce(IV) to the porphyrin to form an oxazine ring followed by the formation of the isoporphyrin intermediate. However, direct evidence for the nucleophilic attack of water(hydroxyde) to the Cmpd I-like species points to the mechanism proposed in Figure 2. (b) Attempts to isolate the isoporphyrin intermediates from an organic solution (CH_2Cl_2) to be further oxidized by CAN, as a differing approach to corroborate our proposed mechanism of reaction, were unsuccessful due to their instability in aqueous solutions at room temperature (see also SI). (c) Further evidence for the proposed mechanism was obtained by the use of methanol as nucleophile in methanol:water and methanol:acetonitrile mixtures, observing incorporation of MeO^- into the benzoyl-billiverdin complex (1 + (O) (OMe)) and also in the final products (TA + (O)(OMe)) and (TA + (OMe)₂) from the two different solvent systems, respectively (see Figures S30 and S31).

(12) Takahashi, A.; Kurahashi, T.; Fujii, H. *Inorg. Chem.* **2011**, *50*, 6922.

(13) (a) Wang, J.; Niemevz, F.; Lad, L.; Huang, L.; Alvarez, D. E.; Buldain, G.; Poulos, T. L.; Ortiz de Montellano, P. R. *J. Biol. Chem.* **2004**, *279*, 42593. (b) Evans, J. P.; Niemevz, F.; Buldain, G.; Ortiz de Montellano, P. R. *J. Biol. Chem.* **2008**, *283*, 19530. The authors proposed that an isoporphyrin intermediate could be observed when a phenyl-substituted heme was used as cofactor/substrate, since C–C cleavage is then not favored. Instead, in the oxidation of hemin, an isoporphyrin is not observed because fast rearomatization just implies that a proton loss occurs.

(14) A reviewer suggested that alternative formulations of the 615 nm intermediate are possible, and this should be considered.

(15) Nakajima, R.; Yamazaki, I. *J. Biol. Chem.* **1980**, *255*, 2067.

(16) Matsui, T.; Nambu, S.; Ono, Y.; Goulding, C. W.; Tsumoto, K.; Ikeda-Saito, M. *Biochemistry* **2013**, *52*, 3025.